Journal of Thermal Analysis and Calorimetry, Vol. 77 (2004) 207–216

OXIDATION KINETICS STUDY OF THE IRON-BASED STEEL FOR SOLID OXIDE FUEL CELL APPLICATION

T. Brylewski[*]*, J. Dąbek and K. Przybylski*

Department of Solid State Chemistry, Faculty of Materials Science and Ceramics,
AGH University of Science and Technology, al. Mickiewicza 30, 30-059 Krakow, Poland

Abstract

Kinetics of oxidation of Fe-Cr steel containing 25 wt.-percent Cr was studied as a function of temperature (1023–1173 K) for up to 480 h in flowing air, which corresponds to SOFC cathode environment operating conditions. The oxidation process was found to be a parabolic, suggesting that the diffusion of ionic defects in the scale is the slowest, rate determining step and it occurs predominantly by short-circuit diffusion paths. Comparison of the determined activation energy of oxidation of the studied steel with literature data indicates that at 1098–1173 K the chromia scale grows by the outward solid-state diffusion of chromium interstitials, whereas at 1023–1098 K – through a significant contribution of counter-current oxygen/chromium diffusion along Cr_2O_3 grain boundaries. The oxide scales were composed mainly of Cr_2O_3 with a continuous thin $Mn_{1.5}Cr_{1.5}O_4$ spinel layer on top of the chromia scale. The oxidation test results on Fe-25Cr steel demonstrate the applicability of the commercial type DIN 50049 stainless steel as interconnect for SOFC.

Keywords: chromia scale, Fe-Cr steel, kinetics, microstructure, oxidation, SOFC interconnect

Introduction

The high-temperature oxidation of high-Cr iron-based steel has been recently studied extensively. This interest arises from the possibility of the application of this steel to the metallic-type of interconnect in Solid Oxide Fuel Cell (SOFC) operating at 1073 K [1–7]. The interconnect is one of the critical components of the planar-type high-temperature SOFC, which separates the cathode and the anode gases and provides the electrical connection between the single cells in the stack [7]. The key issue of the chromia-forming Fe-Cr steel application is its good corrosion resistance, its thermal expansion coefficient which is close to that of solid electrolytes of stabilized zirconia and the ability to work efficiently in air and in H_2-H_2O gas mixture due to the high oxidation resistance of the thermally grown chromia scale [1–8].

The examined ferritic stainless steel exhibits high temperature resistance owing to the presence of alloying additions such as Cr, Mn, Si, which improve the scale adhesion. Furthermore, the electrical resistivity across the oxide scale development

* Author for correspondence: E-mail: brylew@uci.agh.edu.pl

1388–6150/2004/ $ 20.00

Akadémiai Kiadó, Budapest
Kluwer Academic Publishers, Dordrecht

during the oxidation process of the steel should be kept at a low level, accordingly to the main requirements for SOFC interconnect materials [7]. Thus, in order to evaluate the predicted change with time in the electrical resistivity of the scale formed on the steel it is necessary to understand in detail the kinetics and the mechanism of the formation of the heterogeneous layer of the scale on such multicomponent steel.

In the present work the investigations of the oxidation kinetics and mechanism as well as microstructure development of scales formed on Fe-25 wt.-% Cr steel in air, corresponding to the cathode operating conditions of SOFC, are discussed in terms of applicability as an interconnect in the planar-type SOFC.

Experimental

Commercial type DIN 50049 stainless steel (Valcovny Plechu a.s. Frydek-Mistek, Czech Republic) with chemical composition of Fe-73.35; Cr-24.55; Mn-0.28; Si-0.74; Ni-0.99; C-0.04 in mass % was tested. A coupon of 10×20×0.5 mm^3 was abraded with silicon carbide paper down to #1500-grid, then mirror finished with 2 μm alumina slurry followed by ultrasonic degreasing in acetone, and dried before oxidation test.

Isothermal oxidation kinetics study of Fe-25Cr steel was carried out in an automatic electronic Vacuum Head Microbalance type MK2-G5 (CI Electronics Ltd., UK) described elsewhere [4] at temperature range of 1023–1173 K for 70 up to 480 h in dry, flowing air (300 $cm^3\ min^{-1}$) at 1 atm pressure. The mass changes of the samples were measured with the sensitivity of 0.1 μg.

To monitor the development of the microstructures and morphologies of oxide scales formed under different conditions of experiment, the scanning electron microscopy (SEM) equipped with energy dispersive X-ray analysis (EDS) using a JEOL JSM-5400, and reflection X-ray diffraction analysis (Philips X'Pert Pro) were applied.

Results and discussion

Oxidation kinetics

The oxidation reactions of Fe-25Cr steel were found to be a parabolic over the applied temperature range. The results of the selected kinetics curves of the mass gain per unit area as a function of time for isothermal oxidation of Fe-25Cr steel in air at various temperatures are shown in Fig. 1. The obtained kinetics data reveal a relatively low oxidation rate of the studied steel at different temperatures, confirming its high corrosion resistance. Some irregularities in the kinetics profile, according to small mass losses, probably due to scale spallation for steel oxidized at various temperatures, are noticeable. Moreover, a change from a slow initial nonparabolic stage to the parabolic one after approximately from 10 to 70 h of reaction in selected experimental oxidation conditions were observed (Fig. 1).

The values of the parabolic rate constant (k_p) were determined by the mass gain per unit surface area of a specimen $\left(\frac{\Delta m}{A}\right)$ and exposure time (t);

$$\left(\frac{\Delta m}{A}\right)^2 = k_p t \quad (1)$$

where k_p is the parabolic rate constant. The k_p was obtained from the slope of a linear regression-fitted line of $\left(\frac{\Delta m}{A}\right)^2$ *vs. t* plot. The results of these calculations are listed in Table 1 and illustrated graphically in the form of the mass change per unit squared as a function of time in Fig. 2.

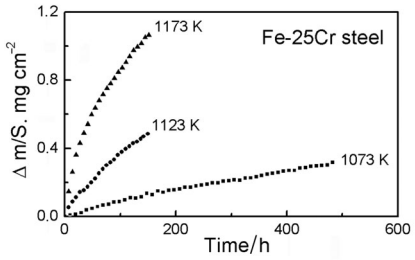

Fig. 1 Oxidation kinetics of Fe-25Cr steel in air at several temperatures

Table 1 Parabolic rate constants (k_p) and the correlation coefficients (r) in regression analysis of Fe-25Cr steel oxidation in air

T/K	Oxidation time/h	k_p/g^{2}cm^{-4}s^{-1}	r
1023	0–150	$1.35\cdot10^{-14}$	0.9649
1048	20–190	$5.05\cdot10^{-14}$	0.9816
1073	70–310	$4.94\cdot10^{-14}$	0.9933
	310–480	$8.00\cdot10^{-14}$	0.9935
1098	0–90	$3.46\cdot10^{-13}$	0.9973
1123	20–150	$7.07\cdot10^{-13}$	0.9995
1148	0–70	$1.28\cdot10^{-12}$	0.9870
1173	10–150	$2.17\cdot10^{-12}$	0.9998

The calculated parabolic rate constants for the oxidation of Fe-25Cr steel at 1023-1173 K were of the order of 10^{-12} to 10^{-14} g^2 cm^{-14} s^{-1}, which are typical of chromia-formers [8]. It follows from the plot (Fig. 2) and the data (Table 1) that the small difference in values of the two determined parabolic rate constants, according to slight deviation of the total mass change initiated at 310 h for the behavior of Fe-25Cr steel oxidized in 1073 K, was a symptom of 'breakaway' type oxidation, as discussed later.

The parabolic rate constant of oxidation was found to be an exponential function of temperature, according to Arrhenius equation:

$$k_p = k_0 \exp\left(\frac{-E_a}{RT}\right) \quad (2)$$

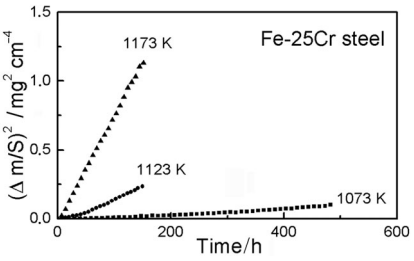

Fig. 2 Parabolic plots of the oxidation for Fe-25Cr steel at 1073 K

Table 2 Data of activation energies (E_a) and pre-exponential constants (k_0) for the oxidation of pure Cr and Fe-Cr alloys

Materials	E_a/kJ mol^{-1}	k_0/g^{2}cm^{-4} s^{-1}	T_{range}/K	Ref.
Cr	247	$1.1\cdot10^{-1}$	973–1473	9
Fe-20Cr alloy	201	$1.0\cdot10^{-2}$	923–1223	12
Fe-16Cr steel	202.3	$6.8\cdot10^{-4}$	1023–1173	5
Fe-25Cr steel	260	$8.8\cdot10^{-1}$	1098–1173	Present work
	380	$3.7\cdot10^{5}$	1023–1098	
Cations in Cr_2O_3	255	$1.4\cdot10^{-1}$[cm^2 s^{-1}]	1323–1723	10
Anions in Cr_2O_3	423	16[cm^2 s^{-1}]	1373–1723	13

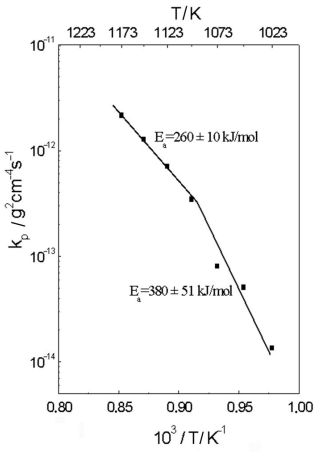

Fig. 3 Temperature dependence of parabolic rate constant for oxidation of Fe-25Cr steel

where k_o is the pre-exponential factor, E_a is the activation energy, R is the gas constant and T is the absolute temperature. In Fig. 3 the dependence of the parabolic rate constant of oxidation on temperature for Fe-25Cr steel is presented. The determined

activation energy from Eq. (2) in the temperature range of 1098–1173 K was equal to 260±10 kJ mol^{-1} and it increased to the value of 380±51 kJ mol^{-1} for lower oxidation temperature range of 1023–1098 K (Fig. 3). To compare the experimental values of the activation energies (E_a) and the pre-exponential constant (k_o) with literature data, Table 2 lists these values, together with data for diffusion in chromia. It has been stated that the present experimental activation energy of 260±10 kJ mol^{-1} agrees with the corresponding results for pure Cr oxidation at different pressures, and for cation self-diffusion in Cr_2O_3 [9, 10]. Thus the rate of oxidation for the present steel is controlled by the outward solid-state diffusion of Cr cation interstitials in the chromia scale, which becomes increasingly important for the lower oxygen pressure [8]. This is also consistent with the literature data [11] according to which the parabolic rate constant for oxidation of chromia-formers is independent of oxygen partial pressure at temperatures below about 1300 K. In addition, it has been found that the present experimental values of the parabolic rate constants for the growth of polycrystalline chromia scale on Fe-25Cr steel in the whole temperature range were by about five orders of magnitude higher than the calculated values from the lattice diffusion data [11]. This strongly suggests that the diffusion in Cr_2O_3 occurs predominantly by short-circuit diffusion paths [8, 11].

As regards the value of activation energy of 380±51 kJ mol^{-1}, for oxidation temperature range of 1023–1098 K it has been proposed that the mechanism of formation of the oxide scale is governed by the counter-current chromium and oxygen diffusion through Cr_2O_3 grain boundaries, being an important transport path [8]. The relative value of E_a was approximately consistent with the corresponding results for anion self-diffusion in Cr_2O_3 (Table 2) within the limit of the standard error in the experimental activation energy of about ±51 kJ mol^{-1}. Evidence for oxygen transport contribution through Cr_2O_3 scales was the presence of convoluted scale configuration developed on the studied steel during the scale-growth process involving concurrent transport of chromium and oxygen, as discussed later.

Scale structure, morphology and composition

The oxidation of Fe-25Cr alloys results in the formation of a double-layered scale. The X-ray diffraction analyses performed on the top of the reaction products formed on several samples after oxidation at various thermal conditions have indicated that the structure of the scale consists mainly of Cr_2O_3. The spinel phase of composition close to $Mn_{1.5}Cr_{1.5}O_4$ and iron rich Fe-Cr solid solution with α-Fe type structure originating from the substrate material was also identified. Figure 4 shows the X-ray pattern, for instance, obtained for sample exposed in air at 1123 K for 150 h. Examination of the scale microstructure through the SEM observation in connection with EDS analysis has revealed that the inner layer of the oxide scales formed on the studied steel throughout the whole range of experimental conditions was composed of Cr_2O_3 doped with Fe. The outer layer was built of $Mn_{1.5}Cr_{1.5}O_4$ spinel. Morphology observation has shown that the surface of the scales obtained after oxidation of Fe-25Cr steel in air at 1023–1173 K was flat, but with some thick nodular growths

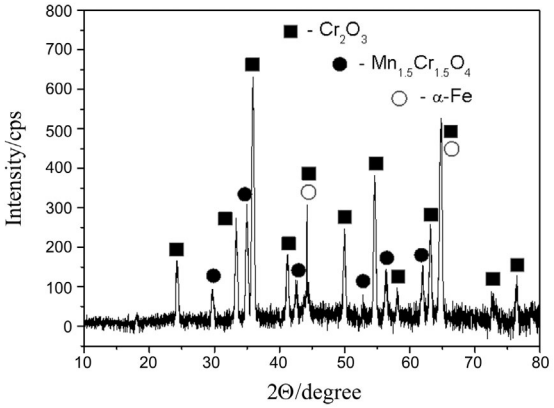

Fig. 4 X-ray diffraction pattern of scale on Fe-25Cr steel oxidized at 1123 K for 150 h

and string-like precipitations of a preferred orientation. Moreover, scale convolution developed on a certain area of the oxidized samples was visible. Matrix of the oxide scale was composed of fine-grained structure and its morphology changed as the oxidation proceeded.

Figure 5 shows the external surfaces of a scale after oxidation in air at 1023–1173 K, exhibiting rather uneven areas composed of non-uniform oxide grains with nodule-like oxides. After exposure at 1023 K for 190 h a small fine-grained matrix composed of chromia coarse-grain with visible paths rich in chromium and iron, as indicated by EDS analysis, was observed (Fig. 5a). Besides a large conglomeration of (Cr, Fe)-rich corundum-type oxide, there were also a few (Cr, Mn)-spinel type oxide nodules at the early stages formation, which developed as an outgrowth from a Cr_2O_3 ridge (Fig. 5a). Figure 5b shows the surface of some cracks initiating the scale layer spallation at 310 h (Fig. 2). The whole of the surface was covered with a coarse-grain layer composed of $Mn_{1.5}Cr_{1.5}O_4$ spinel with several thick nodular growths (Fig. 5b). These nodules of about 2–18 μm in diameter were $Mn_{1.5}Cr_{1.5}O_4$ spinel, the presence of which was confirmed by EDS and XRD analyses. The corresponding semi-quantitative EDS spectrum taken from the analyzed nodules is given in Fig. 6. During oxidation in air at the highest experimental temperature of 1173 K, a relatively angular tetrahedral form of spinel crystallites of approximate composition of $Mn_{1.5}Cr_{1.5}O_4$ on the spinel layer appeared, as can be clearly seen from Fig. 5c.

Systematic morphology observations of the cross-section microstructure of the scales formed on Fe-25Cr steel in air at 1023–1173 K within time range of 70–480 h, show that the scales were compact and had adhesion to metal substrate as well as the thickness of the scale was increased with increasing time in accordance with parabolic law. Figure 7 shows the SEM fracture cross-sectional morphology of the oxide scales formed on Fe-25Cr steel in flowing air at 1073 K for 480 h and at 1173 K for 150 h, respectively. The fine-grained scale of the thickness of about 2.5 μm, and with certain adhesion to the substrate, exhibited a duplex structure of a different chemical

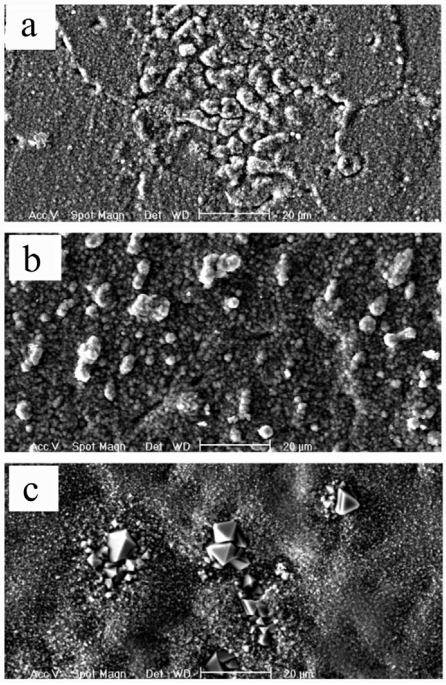

Fig. 5 SEM images of external surfaces of scale formed on Fe-25Cr steel oxidized in air at: a – 1023 K for 190 h; b – 1073 K for 480 h and c – 1173 K for 150 h

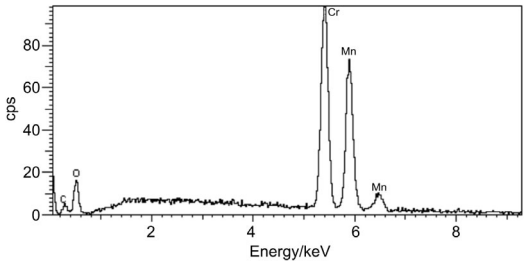

Fig. 6 EDS analysis of spinel nodule

and phase composition (Fig. 7a). The arrangement of the detected phases by the X-ray diffraction analysis was studied in detail using SEM-EDS method. Figure 8 shows the EDS line scan runs for the elements Cr, Mn, Fe, Si and O, performed along the white line visible in Fig. 7a across the metal substrate/oxide scale interface. The X-ray linear microanalysis indicated clearly strong accumulation of Cr and small amount of Fe in the central zone of the thick layer of the scale, reaching the steel substrate, suggesting that this part of the dense layer consists mainly of Cr_2O_3 doped with Fe. The accumulation of Cr and Mn in the outer continuous thin layer is evidence of the formation of spinel of approximate composition of $Mn_{1.5}Cr_{1.5}O_4$. The

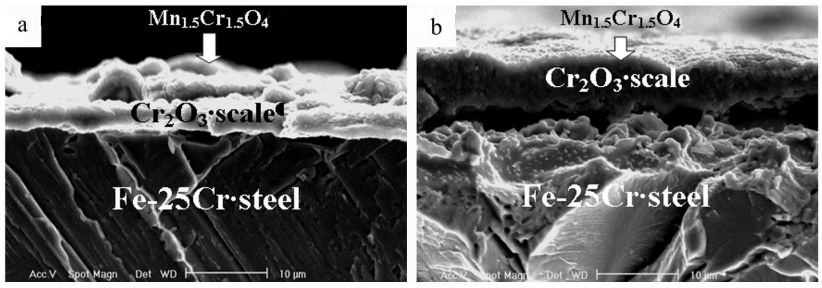

Fig. 7 SEM micrographs of fracture cross-section of the oxide scales formed on Fe-25Cr steel in air at: a –1073 K for 480 h and b – 1173 K for 150 h

contribution of the spinel layer in the chromia Fe-doped scale was confirmed by EDS analysis (Fig. 8). The mechanism of formation of $Mn_{1.5}Cr_{1.5}O_4$ spinel on the top of a Cr_2O_3 layer can be explained by both thermodynamic stability of this compound in the applied experimental conditions and by very fast diffusion of manganese in the chromia scale according to the suggestions of Cox [14] that diffusion coefficients of metals decrease in order $D_{Mn} > D_{Fe} > D_{Cr}$ assuming that these metals diffuse as ions via Cr^{3+} - lattice sites in Cr_2O_3. Thus, because of slower Cr diffusivity, the inner part of the scale is composed only of chromia doped with Fe, while Mn diffuses more rapidly than Fe and it is enriched close to the scale/gas interface and thereby forming a continuous spinel layer. Previous experimental data concerning the influence of Mn

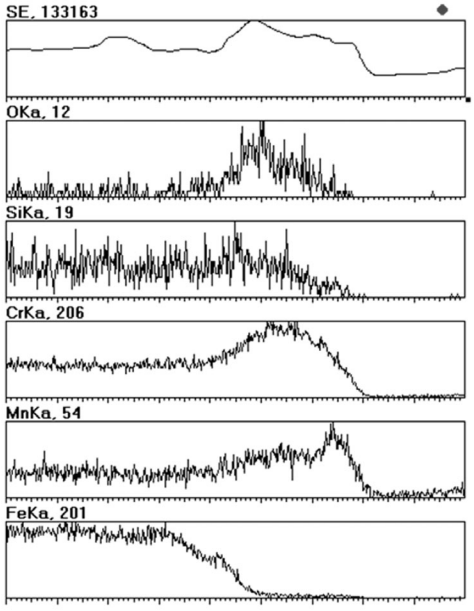

Fig. 8 EDS line scan runs along the white line in Fig. 7a across the scale/metal interface

alloying addition on oxidation properties strongly suggested that an insufficient Mn addition of steel (below 1.0 mass%) results in the Cr depleted zone on the substrate side of the oxide-substrate interface and thereby leads to spallation of the increased Cr_2O_3 layer during oxidation process [15]. In case of the studied steel, containing 0.28 mass% of Mn, formation of a thin protective spinel oxide layer outside Cr_2O_3 scale cannot fully suppress the occurrence of breakaway. However, it has been found that the oxide scale adherence was improved by the presence of the subscale oxide precipitates of amorphous SiO_2, due to the internal oxidation of the alloying addition of Si. The existence of such inclusions at the oxide/metal interface was confirmed by slight increase of the element Si in the line scan profile shown in Fig. 8. As it can be clearly seen from Fig. 7a, the developed scale on the studied steel at 1073 K exhibits a small convoluted configuration. This morphological effect may thereby lead to large growth stresses and often to the development of small cracks as a result of the counter-current diffusion of chromium and oxygen with the predominance contribution of the latter [8]. After exposure of the studied steel to air at 1173 K for 150 h, the developed scale had approximately uniform thickness of about 6 μm, was compact and exhibited large voids (Fig. 7b). The presence of such voids at scale/metal interface was associated with a major contribution of outward solid-state diffusion of Cr-cations in the chromia scale, which is the rate-determining step in the overall process of Cr_2O_3 scale growth on Fe-25Cr steel in accordance with equation (1).

From the practical point of view for the application of Fe-25Cr steel to construct interconnect, the formation of $Mn_{1.5}Cr_{1.5}O_4$ spinel on chromia scale is desirable because of its higher electrical conductivity than that of chromia layer [8]. Moreover, manganese spinel shows lower Cr evaporation rate than Cr_2O_3 [8]. The formation mechanism of the chromia layer is also an important feature in the oxidation behavior of Fe-25Cr steel, which will be taken into account as it has significant influence on the electrical contact between the metal and oxide scale and thereby on the creation of the conditions for a prolonged exploitation of metallic interconnect in SOFC.

Conclusions

- The oxidation of the examined Fe-25Cr steel follows the parabolic rate law within temperature range of 1023–1173 K i.e., the rate of oxidation of the steel is controlled by solid-state diffusion.
- The calculated parabolic rate constant for Fe-25Cr steel oxidation in flowing air at 1023–1173 K was of the order of 10^{-12} to 10^{-14} g^2 cm^{-14} s^{-1}, typical of chromia-formers, and by about five orders of magnitude higher than the calculated values from the lattice diffusion data. This suggests that the diffusion in the scale occurs predominantly by short-circuit diffusion paths.
- The calculated activation energy of oxidation of the studied steel at 1098–1173 K is in satisfactory agreement with those for pure Cr and cation self-diffusion in Cr_2O_3 indicating that the chromia scale grows by the outward solid-state diffusion of Cr cation interstitials, whereas the determined activation energy for oxidation temperature range

of 1023–1098 K suggests the counter-current oxygen/chromium diffusion of oxygen through Cr_2O_3 grain boundaries.
- The oxide scales which develop on Fe-25Cr steel during oxidation were composed mainly of Cr_2O_3 doped with Fe. Additionally, the appearance of a continuous thin $Mn_{1.5}Cr_{1.5}O_4$ spinel layer on top of the chromia scale and of the internal oxide inclusions probably due to SiO_2 was found.
- The commercial type DIN 50049 stainless steel is a promising metallic material for the construction of interconnects used in the planar type of the solid oxide fuel cell.

* * *

Financial support from the Polish State Committee for Scientific Research (KBN), Project No. 4 T08D 014 22 is gratefully acknowledged.

References

1 W. J. Quaddakkers, H. Greiner and W. Köck, Proceedings 1st European Solid Oxide Fuel Cell Forum, Lucerne, Switzerland, European SOFC Forum Secretariat, Baden, Switzerland, 1994, p. 525.
2 T. Kadowaki, T. Shiomitsu, E. Matsuda, H. Nakagawa, H. Tsuneizumi and T. Maruyama, Solid State Ionics, 67 (1993) 65.
3 L. Mikkelsen, P. H. Larsen and S. Linderoth, J. Therm. Anal. Cal., 64 (2001) 879.
4 K. Przybylski, J. Prażuch, T. Brylewski and T. Maruyama, Proceedings 14th International Corrosion Congress, CorrISA, Cape Town, South Africa, Vol. 2, 1999, p. 1.
5 T. Brylewski, M. Nanko, T. Maruyama and K. Przybylski, Solid State Ionics, 143 (2001) 131.
6 W. Z. Zhu and S. C. Deevi, Mat. Sci. Eng., A 348 (2003) 227.
7 N. Q. Minh and T. Takahashi, Science and Technology of Ceramic Fuel Cells, Elsevier, Amsterdam 1995.
8 P. Kofstad, High Temperature Corrosion, Elsevier, New York 1988.
9 W. C. Hagel, Trans. Am. Soc. Metals, 56 (1963) 583.
10 W. C. Hagel and A. W. Seybolt, J. Electrochem. Soc., 108 (1961) 1246.
11 K. Przybylski and G. J. Yurek, Mater. Sci. Forum, 43 (1989) 1.
12 D. Mortimer and W. B. A. Sharp, Br. Corros. J., 3 (1968) 61.
13 W. C. Hagel, J. Am. Ceram. Soc., 48 (1965) 70.
14 M. G. E. Cox, B. McEnanay and V. D. Scott, Phil. Mag., 26 (1972) 839.
15 M. Oku, S. Nakamura and N. Hiramatsu, Mater. High Temp., 18(S) (2001) 153.